VI International Conference on Computational Methods for Coupled Problems in Science and Engineering
COUPLED PROBLEMS 2015
B. Schrefler, E. Oñate and M. Papadrakakis(Eds)

SIMULATION OF CONSOLIDATION IN LARGE STRAINS: A COMPARISON BETWEEN FINITE ELEMENT METHOD AND MATERIAL POINT METHOD

N. Spiezia†, F. Ceccato†*, V. Salomoni†, P. Simonini†

†Department of Civil, Environmental and Architectural Engineering (DICEA)
University of Padua
Via Marzolo 9, 35131 Padova, Italy
e-mail: francesca.ceccato@dicea.unipd.it

Key words: Large strains, consolidation, Finite Element, Material Point Method

Abstract. The numerical simulation of a consolidation process undergoing large strains is a challenging task that requires the formulation and the solution of the coupled solid-deformation/fluid-diffusion problem within a changing geometry. Deformations can be rigorously taken into account with the classical Finite Element Method (FEM) based on continuum mechanics of porous media at finite strains. Alternatively, several innovative methods (SPH, MPM, PFEM, MLPG, etc.), which have been specifically developed to simulate large deformations, can be used. Among them, the Material Point Method (MPM) has been recently grown in popularity. With the MPM, large deformations are simulated with material points (MP) moving through a fixed mesh. The MP trace all the properties of the continuum (mass, velocity, stress, strain as well as external loads), while the mesh is used to solve the governing equations, but does not store any permanent information thus it can be redefined at the end of each time step, preventing problems of element distortions. The aim of this work is to investigate the analogies and the differences in terms of theoretical formulation and numerical results between FEM and MPM in consolidation processes undergoing large deformations. In fact, the simulations of the one-dimensional consolidation process in case of small deformations demonstrate that the two methods give identical results, which are also in agreement with the analytical solution demonstrated by Terzaghi. On the contrary, differences are observed in the case of large deformations. The results obtained with the two formulations are compared and discussed, enlightening the most probable source of differences.

1 INTRODUCTION

The numerical simulation of consolidation processes is a fundamental task, which can have important implications in the design of geotechnical structures. The simulation

of these phenomena, which involve the coupled interaction between the solid and the fluid phases, becomes particularly challenging when the solid phase is subjected to large strains, introducing a source of geometric non linearity in the formulation. There are many classical geotechnical applications where the finite deformations effects on a consolidation process could critically influence the results of a numerical analysis. For example, the consolidation in highly compressible clays, or the consolidation under a tower, due to the $P - \delta$ effect [1].

The consolidation process can be accurately simulated using the classical coupled finite element formulation, based on continuum theory of mixtures, considering the soil-water mixture as a two-phase continuum. Finite strains can be rigorously taken into account as an extension of the infinitesimal framework [1, 2], adopting an adequate formulation for the constitutive model. However, Updated Lagrangian Finite Element Methods (UL-FEM) encounter numerical problems for severe element distortions, with the consequent lack of convergence of the algorithm.

The problem of severe mesh distortion in UL-FEM may be circumvented by remeshing the domain or refining the regions where the elements are most deformed [3, 4]. Alternatively, some stabilization techniques have been proposed to prevent excessive element distortion [5, 6]. These strategies have the disadvantage to increase considerably the computational cost; moreover, numerical stability is still not ensured in case of extreme distortions.

To overcome the distortion problems encountered by FEM undergoing large deformations, in the last decades several innovative methods have been proposed in the literature, such as SPH [7], MPM [8], PFEM [9], MLPG [10]. In particular, the Material Point Method (MPM) has been recently grown in popularity.

The MPM belongs to the family of particle-based methods. It derives from the Particle-in-cell method (PIC) used for fluid mechanics [11]. Schreyer, Sulsky and co-workers, extended it for problems of solid mechanics [8]. Since then, the method has been widely applied to many fields of engineering and science and extended with advanced features. The application of MPM to multiphase problems is recent [12–17] and the research is in progress.

Although the MPM has been successfully applied to study coupled large deformation problems [18–20], not much work has been done to compare the numerical results obtained with the FEM based on finite strain theory and the MPM, in particular to simulate large deformation phenomena.

This work investigates the analogies and the differences in terms of theoretical formulation and numerical results between the FEM and MPM, in consolidation process undergoing large deformation. These methods give identical results in case of small deformation, coincident with the classical Terzaghi's solution. On the contrary, differences are observed in case of large deformations. The goal of this study is to identify the possible sources of differences, suggesting a discussion on the topic likely leading to future improvements of the methods.

The article is organized as follow. Section two and three briefly introduce respectively the FEM and MPM formulation. Section four presents the numerical results obtained by the two methods. One-dimensional consolidation with elastic and elasto-plastic material is solved, in case of small and large deformations. Section five draws the conclusion, discussing the differences among the two methods.

2 FINITE ELEMENT FORMULATION

This section recalls the complete set of governing equations, which allow for the solution of quasi-static deformation-diffusion boundary-value problems, such as consolidation, based on the classical mixture theory [21, 22].

Let $\boldsymbol{x} = \varphi(\boldsymbol{X}, t)$ denote the position of the solid material point X and $\boldsymbol{F} = \partial \boldsymbol{x}/\partial \boldsymbol{X}$ the associated deformation gradient of the solid matrix, with the Jacobian J such that $J = \det(\boldsymbol{F}) = \mathrm{d}v/\mathrm{d}V$. We denote the volume fraction ϕ^α of the constituent α as the ratio between its volume $\mathrm{d}V^\alpha$ divided by the total volume of the mixture $\mathrm{d}V$, that is, $\phi^s = \mathrm{d}V^s/\mathrm{d}V$ and $\phi^w = n = \mathrm{d}V^w/\mathrm{d}V$, with n denotes the porosity. Therefore,

$$\phi^s + \phi^w = 1 \tag{1}$$

The partial mass density of constituent α is given by $\rho^\alpha = \phi^\alpha \rho_\alpha$, where ρ_α is the intrinsic mass density of constituent α. This gives

$$(1-n)\rho_s + n\rho_w = \rho^s + \rho^w = \rho \tag{2}$$

where ρ is the total mass density of the mixture.

With these preliminaries, the conservation of mass equation for the solid and water phases are respectively

$$\dot{\rho}^s + \rho^s \nabla^{\boldsymbol{x}} \cdot \boldsymbol{v} = 0; \tag{3}$$

$$\dot{\rho}^w + \rho^w \nabla^{\boldsymbol{x}} \cdot \boldsymbol{v} = -\boldsymbol{\nabla}^{\boldsymbol{x}} \cdot \boldsymbol{q}, \tag{4}$$

where $\boldsymbol{\nabla}^{\boldsymbol{x}} \cdot (\cdot)$ is the divergence operator with respect to the current configuration, $\boldsymbol{v}$ is the velocity of the solid phase, $\boldsymbol{w}$ is the velocity of the water phase, $\boldsymbol{q} \equiv \rho^f \tilde{\boldsymbol{v}} = \rho^w(\boldsymbol{w} - \boldsymbol{v})$ is the Eulerian relative flow vector of the water phase with respect to the solid matrix. Adding Eqs. (3) and (4), we get the basic conservation of mass equation for the system, i.e.

$$\dot{\rho}_0 = -J \nabla^{\boldsymbol{x}} \cdot \boldsymbol{q}, \tag{5}$$

where $\rho_0 \equiv J\rho$ is the pull-back mass density of the mixture in the reference configuration.

Ignoring inertial forces, the balance of linear momentum in Lagrangian form can be written as

$$\nabla^{\boldsymbol{X}}(\boldsymbol{P}) + \rho_0 \boldsymbol{g} = \boldsymbol{0}. \tag{6}$$

where $\boldsymbol{g}$ is the gravity vector. The first Piola-Kirchhoff stress tensor $\boldsymbol{P}$ reads

$$\boldsymbol{P} = \boldsymbol{\tau} \cdot \boldsymbol{F}^{-T} = \boldsymbol{\tau}' \cdot \boldsymbol{F}^{-T} - \theta_w \boldsymbol{F}^{-T} \tag{7}$$

where $\boldsymbol{\tau} = J\boldsymbol{\sigma}$ is the symmetric total Kirchhoff stress tensor, $\boldsymbol{\tau}' = J\boldsymbol{\sigma}'$ is the effective Kirchhoff stress tensor and $\theta_w = Jp_w$ is the Kirchhoff pore pressure, in accordance with the principle of effective stress.

The links between the state of stress and the deformations and between the flow vector and the water pressure in the porous media are provided by constitutive relationships. The stresses are assumed to be a nonlinear function of the deformations via an elastoplastic constitutive response. On the other hand, the relative flow vector is related to the fluid pressure using Darcy's law, assuming constant permeability. The constitutive law for the solid phase is cast within the framework of nonlinear kinematics where the total deformation gradient is assumed to allow the multiplicative decomposition into elastic and plastic parts, $\boldsymbol{F} = \boldsymbol{F}^e \cdot \boldsymbol{F}^p$, where $\boldsymbol{F}^e$ and $\boldsymbol{F}^p$ are defined as the elastic and plastic deformation gradient, respectively. The constitutive law is given in terms of the Kirchhoff effective stress tensor $\boldsymbol{\tau}'$ and the left elastic Cauchy-Green deformation tensor $\boldsymbol{b}^e = \boldsymbol{F}^e \cdot \boldsymbol{F}^{eT}$ through the relation

$$\boldsymbol{\tau}' = 2\frac{\partial \Psi}{\partial \boldsymbol{b}^e} \cdot \boldsymbol{b}^e. \tag{8}$$

where Ψ is the strain-energy function.

The balance laws (5) and (6), together with constitutive relations, provide a complete set of governing equations, which allow for the solution of quasi-static deformation-diffusion boundary-value problems. The discretized equations are obtained following standard Galerkin procedure, approximating the nodal displacements $\boldsymbol{u}$ and pore pressure p_w by means of shape functions ($\boldsymbol{N}$, $\boldsymbol{N}^p$), and integrating implicitly over time. Hence, the two balance equations can be written as

$$\boldsymbol{H}^{ext} - \boldsymbol{H}^{int}(\boldsymbol{u}, p_w) = \boldsymbol{0} \tag{9}$$

$$\boldsymbol{F}^{ext} - \boldsymbol{F}^{int}(\boldsymbol{u}, p_w) = \boldsymbol{0} \tag{10}$$

where $\boldsymbol{H}^{int} = \int_{V_0} [\boldsymbol{N}^{pT} \Delta\rho_0 - \Delta t(J\boldsymbol{\Gamma}^T \boldsymbol{q})] \mathrm{d}V_0$ and $\boldsymbol{F}^{int} = \int_{V_0} [\boldsymbol{B}^{\boldsymbol{T}}(\boldsymbol{\tau}' - Jp_w\boldsymbol{I}) - \rho_0 \boldsymbol{N}^T \boldsymbol{g}] \mathrm{d}V_0$. For more details the reader should refer to [1, 2].

3 THE MATERIAL POINT METHOD

In the MPM, arbitrary large deformations of a body are simulated by a set of material points (MP) which move through a computational finite element mesh. The MP carries all the information of the continuum such as velocity, acceleration, stress, strain, material parameters as well as external loads. It can be regarded as an extension of the FEM, because the underlying finite element grid is used, as with the FEM, to solve the system

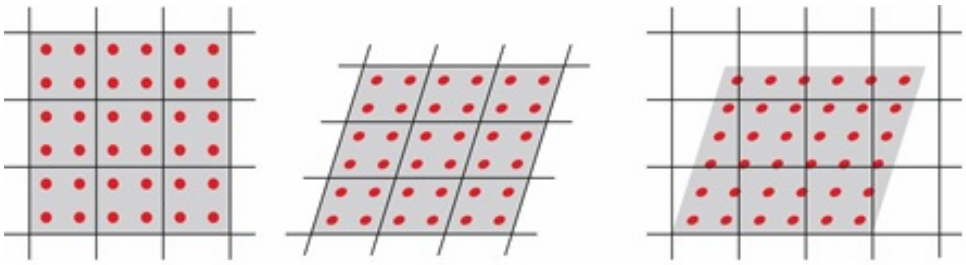

Figure 1: (left) configuration at the beginning of a time step in which the red dots are the MP; (center) incrementally deformed mesh; (right) reset mesh at the end of a time step

of equilibrium equations. However, information is mapped from nodes to MP at the end of each time step and the mesh is usually reset into its original state (Fig. 1). The mesh does not follow the deformations of the body as in the FEM, thus preventing problems of element distortion.

An available dynamic MPM code is used in this study. The primary unknown variables of the implemented two-phase formulation are the solid velocity $\boldsymbol{v}$ and fluid velocity $\boldsymbol{w}$. This formulation follows [23] and has been preferred for the adopted MPM because it is able to properly capture the dynamic response for general loading [24]. The $(\boldsymbol{v} - \boldsymbol{w})$ formulation is derived from the momentum equations of the water phase and the soil-water mixture as follows. The momentum equation of the water phase is

$$\rho_w \dot{\boldsymbol{w}} + ((n\gamma_w)/k)(\boldsymbol{v} - \boldsymbol{w}) = \nabla p_w + \rho_w \boldsymbol{g} \tag{11}$$

where γ_w is the unit weight of the water and k is the Darcy's permeability; the latter is assumed constant. The second term on the left hand side represents the interaction between solid and fluid.

The momentum equation for the mixture is

$$(1-n)\rho_s \dot{\boldsymbol{v}} + n\rho_w \dot{\boldsymbol{w}} = \nabla \cdot (\boldsymbol{\sigma'} + \boldsymbol{I} p_w) + \rho \boldsymbol{g} \tag{12}$$

where $\boldsymbol{\sigma'}$ is the effective stress and $\boldsymbol{I} = [1, 1, 1, 0, 0, 0]$.

The excess pore pressure increment can be calculated from the mass balance equation for the water phase

$$\dot{p}_w = K_w/n[(1-n)\nabla \cdot \boldsymbol{v} + n\nabla \cdot \boldsymbol{w}] \tag{13}$$

The effective stress increment is calculated with the soil constitutive model as

$$\dot{\boldsymbol{\sigma}}' = \boldsymbol{D}\dot{\boldsymbol{\epsilon}} \tag{14}$$

where $\boldsymbol{D}$ is the constitutive tensor and $\dot{\boldsymbol{\sigma}}'$ is the Jaumann stress rate tensor defined as

$$\dot{\boldsymbol{\sigma}}' = \boldsymbol{\sigma'} - \boldsymbol{W} \cdot \dot{\boldsymbol{\sigma}}' + \dot{\boldsymbol{\sigma}}' \cdot \boldsymbol{W}^{\boldsymbol{T}} \tag{15}$$

in which $\dot{\boldsymbol{\sigma}}$ is the Cauchy stress and $\boldsymbol{W}$ is the spin tensor.

Again, the discretized equations are obtained by deriving the weak form of the momentum conservation, using the Galerkin procedure, and approximating the velocity field by means of shape functions ($\boldsymbol{N}$) [16]. They can be written as

$$\boldsymbol{M_w}\dot{\boldsymbol{w}} = \boldsymbol{F_w^{ext}} - \boldsymbol{F_w^{int}} - \boldsymbol{F_w^{drag}} \tag{16}$$

$$\boldsymbol{M_s}\dot{\boldsymbol{v}} + \bar{\boldsymbol{M}}_{\boldsymbol{w}}\dot{\boldsymbol{w}} = \boldsymbol{F^{ext}} - \boldsymbol{F^{int}} \tag{17}$$

where the subscripts s and w indicate the soil and water phase respectively; no subscript indicates that the quantity belongs to the mixture.

$\boldsymbol{F_w^{drag}} = \int_V n\gamma_w k^{-1}\boldsymbol{N}^T\boldsymbol{N}dV(\boldsymbol{v}-\boldsymbol{w})$ denotes a drag force computed from the relative water velocity $(\boldsymbol{w}-\boldsymbol{v})$ which takes into account the solid-fluid interaction. The mass matrices for the fluid and the soil skeleton are defined as: $\boldsymbol{M}_w = \int_V \rho_w \boldsymbol{N}^T\boldsymbol{N}dV$ and $\boldsymbol{M_s} = \int_V (1-n)\rho_s\boldsymbol{N}^T\boldsymbol{N}dV$. Matrix $\bar{\boldsymbol{M}}_{\boldsymbol{w}}$ is formed using the density $n\rho_w$ in place of ρ_w. For numerical implementation, the lumped mass matrices are used. The internal forces are calculated as $\boldsymbol{F_w^{int}} = \int_V \boldsymbol{B^T I}p_w dV$ and $\boldsymbol{F^{int}} = \int_V \boldsymbol{B^T}\boldsymbol{\sigma}dV$ where $\boldsymbol{\sigma}$ is the total stress. For more details the reader should refer to [16].

In the present study the explicit Euler-Cromer scheme is used. This means that the acceleration is calculated explicitly and the velocity is updated from it implicitly.

The MPM solution procedure follows [25]. The acceleration of the fluid is calculated by solving Eq. (16). It is subsequently used to obtain the acceleration of the solid from Eq. (17). The velocities and the momentum of the MP are updated from the nodal accelerations of each phase. The nodal velocities are then calculated from the nodal momentum and used to compute the strain rate ($\dot{\boldsymbol{\epsilon}}$) at the material point location. The excess pore pressure increment can be calculated from Eq. (13). The effective stress increment is calculated with the soil constitutive model (Eq. 14). The displacement and position of each MP is updated according to the velocity of the solid phase.

4 NUMERICAL RESULTS

The consolidation problem is studied considering a 1m-long column. The head of the column is permeable and the bottom is impermeable, therefore the water can flow out of the column from the top surface and the drainage length h is 1m. Firstly, the case of small deformations is studied and the numerical solution is compared to the Terzaghi's analytical solution. Secondly, large deformations are taken into account. Thirdly, the plastic behavior of soil is considered using the Modified Cam Clay model [26].

In case of small strain, a linear elastic material with Young's modulus $E = 10000kPa$, and Poisson's ratio $\nu = 0$ is used. The permeability is $k = 10^{-3}m/s$. A load of $10kPa$ is applied at the head of the column. In the FEM model the column is discretized with 40 quadrilateral elements, with 9 nodes for the displacements unknowns and 4 nodes for the pressure unknowns, integrated over 9 Gauss Point. On the other hand, in the MPM model the column is discretized with 40 rows of 6 tetrahedral elements containing 4 MP each.

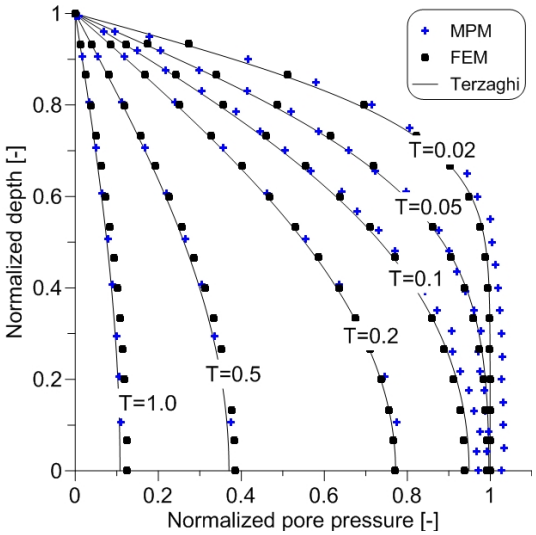

Figure 2: Normalized pore pressure along depth, comparison between numerical and analytical solution.

A non-dimensional time factor can be defined as:

$$T = \frac{c_v t}{h^2} \tag{18}$$

Figure 2 plots the normalized pore pressure p_w/p_{w0} ($p_{w0} = 10kPa$) against the normalized depth y/h as function of the non-dimensional time. The numerical solutions obtained with FEM and MPM are in perfect agreement with the Terzaghi's analytical solution.

The case of large deformations is considered assuming $E = 100kPa$ and applying a load of $\sigma_y = 50kPa$. Figure 3a shows the normalized pore pressure distribution at different normalized time T_L, which calculated with Eq. 18 where h is the initial length of the column. Regarding the pore pressure evolution with time, the MPM predicts higher pore pressures than the FEM, especially for time factors between 0.05 and 0.5. The maximum difference is about 20% at the bottom of the column. Some differences are also observed in the decrease of column height during time (Fig. 3b). In particular, the final column high obtained with the MPM is 0.674m and with the FEM is 0.704m.

The plastic behavior of soil is considered using the modified Cam Clay model with the input parameter summarized in Table 1. The adopted FEM implements the modified Cam Clay model proposed in [27]; the reader should refer to this work for a correct interpretation of the input parameters of the model.

The material is assumed normally consolidated; the initial vertical and horizontal effective stresses are 50kPa. A vertical load of 150kPa is applied. In this case, the consolidation coefficient used to compute the time factor is calculated as:

$$c_v = \frac{k(1+e_0)\sigma'_{v0}}{\lambda\gamma_w} \tag{19}$$

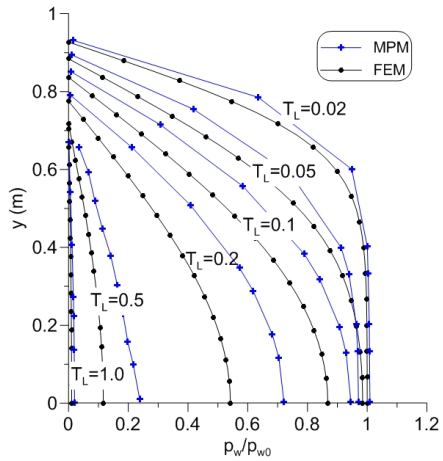

(a) Normalized pore pressure along depth.

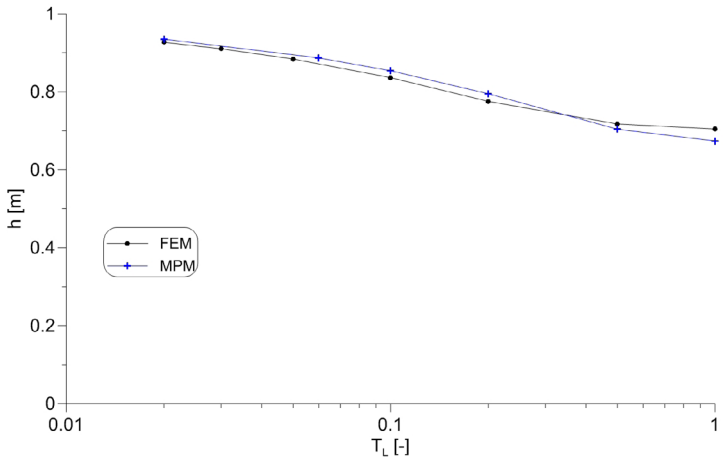

(b) Column height as function of the time factor T_L.

Figure 3: Large strain consolidation with linear elastic material; comparison between MPM and FEM solutions.

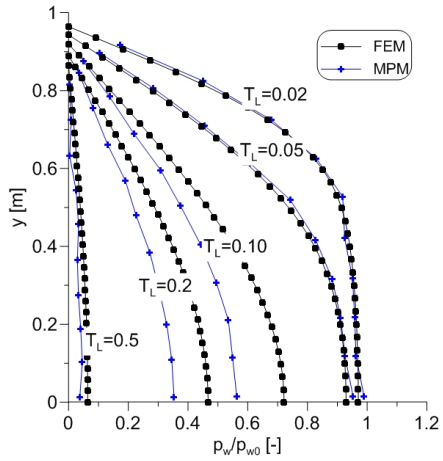

(a) Normalized pore pressure along depth.

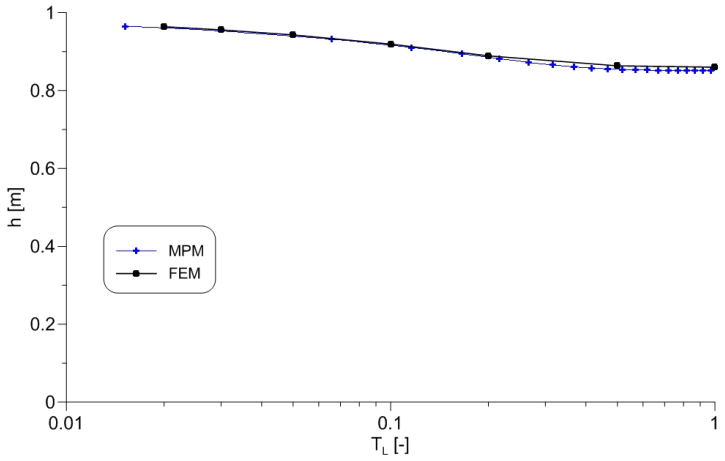

(b) Column height as function of the time factor T_L.

Figure 4: Large strain consolidation with elastoplastic material; comparison between MPM and FEM solutions.

Material property	Symbol	Value
Virgin compression index [-]	λ	0.3
Recompression index [-]	κ	0.04
Effective poisson ratio [-]	ν'	0.25
Slope of CSL in p-q plane [-]	M	0.92
Initial void ratio [-]	e_0	1.0
Darcy's permeability [m/s]	k	$3 \cdot 10^{-3}$

Table 1: Material properties used in CPT analyses with MCC material model

where σ'_{v0} is the initial vertical effective stress.

Figure 4 compares the results obtained with FEM and MPM in terms of pore pressure distribution and column height. With regard to the pore pressure, better agreement is obtained compared to the elastic case. A difference of about 20% is observed for $T_L = 0.10$ and $T_L = 0.2$, while the pore pressure distribution for the other time factors are almost coincident. This peculiar result will be deeply investigated in the near future. The small differences in terms of pressure do not affect significantly the evolution of vertical displacements with time. Both method predict a final settlement of 0.142m.

5 DISCUSSION AND CONCLUSIONS

This paper compares the fully coupled FEM and the MPM in the simulation of one dimensional consolidation undergoing large strains.

Both method, even though adopting different primary unknowns (namely $\boldsymbol{u} - p_w$ and $\boldsymbol{v} - \boldsymbol{w}$), can describe efficiently the solid-displacement/fluid-diffusion process, typical of consolidation problem. Identical results are obtained with the two methods for small deformations. This observation is in agreement with the comparison made in [28] (for harmonic loading and small strain) of the two different ways of coupling solid and fluid interaction. Furthermore, the choice of different primary unknowns involves also the adoption of different time integration algorithms. In fact, the quasi-static FEM adopts an implicit time integration scheme; on the contrary, the dynamic MPM uses an explicit scheme. However, the adopted time increments ensure a sufficiently accurate solution for both methods.

In case of large deformations, the displacements predicted by the two method are in good agreement. However, discrepancies are observed in the evolution of pore pressure distribution.

Probably, the major source of differences between the MPM and the adopted FEM lies in the way large deformations are treated, in particular with respect to the constitutive equations. In MPM the hypothesis of small strain is assumed within the time increment, thus allowing the use of the Jaumann objective stress rate. This formulation restricts the validity of the rate constitutive equation to small elastic strains [29]. As regard the

FEM, the formulation of the constitutive law is based on hyperelasticity combined with the multiplicative decomposition of the deformation gradient. This formulation is more accurate for the development of large elastic strains, and also circumvents the so-called rate issue in finite deformation analysis [27]. The introduction of plasticity reduces the differences between the two methods, because if the elastic strains remain small the results based on the Jaumann rate should be close to results of formulations that are based on the multiplicative decomposition [29].

These considerations do not probably fully explain the differences observed in the pore pressure distributions. Further investigations, focusing on the diffusion problem combined with large deformations, should be carried out, possibly comparing the results with experimental data and also with available analytical solution such as [30].

This paper doesn't accomplish all the aspects in the comparison of the two numerical methods. Since considerable effort has been devoted in the last years to large strain coupled formulation in the MPM, with promising outcomes, a deeper investigation in the results should be carried out. The research should consider bidimensional and three dimensional problems, transient boundary conditions, cyclic loads, etc. In particular, simulations leading to a significant element distortions should be investigated, comparing FEM (enhanced with remeshing techniques) and MPM.

AKNOWLEDGMENTS

The authors thank the MPM research group of Deltares, Delf, The Netherlands for the kind support in the use of the MPM code.

REFERENCES

[1] Borja, R. I., and Alarcon, E., A mathematical framework for finite strain elasto-plastic consolidation. Part 1: balance laws, variational formulation, and linearization *Computer Methods in Applied Mechanics and Engineering* (1995) **122**:145–171.

[2] Borja, R. I., Tamagnini, C., Alarcon, E., Elastoplastic consolidation at finite strain. Part 2: finite element implementation and numerical examples *Computer Methods in Applied Mechanics and Engineering* (1998) **159**:103–122.

[3] Kato, K., Lee N. S., and Bathe, K. J. Adaptive finite element analysis of large strain elastic response *Computers and Structures* (1993) **47**:829–855.

[4] Lee, N.-S. and Bathe, K.-J. Error indicators and adaptive remeshing in large deformation finite element analysis *Finite Elements in Analysis and Design* (1994) **16**:99–139.

[5] Simo, J.C., Armero, F. and Taylor, R.L. Improved versions of assumed enhanced strain tri-linear elements for 3D finite deformation problems *Computer Methods in Applied Mechanics and Engineering* (1993) **110**:359–386.

[6] Nagtegaal, J.C. and Fox, D.D. Using assumed enhanced strain elements for large compressive deformation *International Journal of Solids and Structures* (1996) **33**:3151–3159.

[7] Lucy, L. B. A numerical approach to the testing of the fission hypothesis. *The astronomical journal* (1977) **82**, 1013–1024.

[8] Sulsky, D. Chen, Z. and Schreyer, H.L. A particle method for hystory-dependent materials *Computer Methods in Applied Mechanics and Engineering* (1994) **118**: 179–196

[9] Idelsohn, S., E. Oñate, and F. D. Pin. The particle finite element method: a powerful tool to solve incompressible fows with free-surfaces and breaking waves. *International Journal for Numerical Methods in Engineering* (2004) **61** (7), 964–989.

[10] Atluri, S. and T. Zhu. A new meshless local petrov-galerkin (MLPG) approach in computational mechanics. *Computational mechanics* (1998) **22** (2), 117–127.

[11] Harlow, F. H. *A Machine Calculation Method for Hydrodynamic Problems.* Los Alamos Scientific Laboratory report LAMS-1956.(1955)

[12] Zhang, H., K. Wang, and Z. Zhang. Material point method for numerical simulation of failure phenomena in multiphase porous media. *Computational Mechanics* (2007) p.p. 36–47. Springer.

[13] Zhang, D. Z., Q. Zou, W. B. VanderHeyden, and X. Ma. Material point method applied to multiphase flows. *Journal of Computational Physics* (2008) **227** (6): 3159–3173.

[14] H. W. Zhang, K. P. Wang, and Z. Chen. Material point method for dynamic analysis of saturated porous media under external contact/impact of solid bodies. *Computer Methods in Applied Mechanics and Engineering* (2009) **198**.17 : 1456-1472.

[15] Higo, Y., et al. A coupled MPM-FDM analysis method for multi-phase elasto-plastic soils. *Soils and foundations* (2010) **50**.4:515-532.

[16] Jassim, I. and Stolle, D. and Vermeer, P.Two-phase dynamic analysis by material point method. *International Journal for Numerical and Analytical Methods in Geomechanics* (2013) **37**:2502–2522

[17] Abe, K., K. Soga, and S. Bandara. Material Point Method for Coupled Hydromechanical Problems. *Journal of Geotechnical and Geoenvironmental Engineering* (2013) **140**.3.

[18] Alonso, E.E. and Zabala, F. Progressive failure of Aznalcóllar dam using the material point method, *Géotechnique* (2011) **61** 9: 795–808

[19] Bandara, S.; Soga, K. Coupling of soil deformation and pore fluid flow using material point method. *Computers and Geotechnics* (2015) **63** 199-214.

[20] Ceccato, F., Beuth, L., Vermeer, P. A., Simonini P. Two-phase Material Point Method applied to cone penetration for different drainage conditions. *IS on Geomechanics form micro to macro* (2014) CRC Press - Taylor and Francis Group

[21] Bowen, R.M. *Theory of mixtures*, in: A.C. Eringen (Ed.), Continuum Physics, Volume IIIMixtures and EM Field Theories Academic Press, (1976), New York, NY.

[22] Atkin, R.J. and Craine, R.E. Continuum theories of mixture: basic theory and historical development, *Q. J. Mech. Appl. Math.* (1976) **29**:209-244.

[23] Verruijt, A. *Soil dynamics*. Technische Universiteit, Faculteit Civiele Techniek, 1996.

[24] Van Esch, J., D. Stolle and I. Jassim. Finite element method for coupled dynamic flow-deformation simulation. In 2nd International Symposium on Computational Gaomechanics (COMGEO II), Cavat-Dubrovnik, Croatia (2011).

[25] Al-Kafaji, Issam K. J. *Formulation of a Dynamic Material Point Method (MPM) for Geomechanical Problems*, PhD thesis, University of Struttgart, Germay, 2013

[26] Schofield, A. and P. Wroth. *Critical state soil mechanics*. McGraw-Hill London, 1968.

[27] Borja, R. I., and Tamagnini, C. ,Cam-Clay plasticity Part III: Extension of the infinitesimal model to include finite strains *Computer Methods in Applied Mechanics and Engineering* (1998) **155**:73–95.

[28] Zienkiewicz, O. C., C. T. Chang, and P. Bettess. Drained, undrained, consolidating and dynamic behaviour assumptions in soils. *Geotechnique* (1980) **30**.4 : 385-395.

[29] De Borst, R., Crisfield, M. A., Remmers, J. JC., Verhoosel, C. V. *Nonlinear finite element analysis of solids and structures*. John Wiley & Sons, 2012

[30] Xie, K. H.; Leo, C. J. Analytical solutions of one-dimensional large strain consolidation of saturated and homogeneous clays. *Computers and geotechnics* (2004) **31**.4: 301-314.